IL NUOVO CIMENTO **39 C** (2016) 404
DOI 10.1393/ncc/i2016-16404-9

Colloquia: IWM-EC 2016

Signals of dynamical and statistical process from IMF-IMF correlation function

E. V. Pagano([1])([2]), L. Acosta([3])([4]), L. Auditore([5]), V. Baran([6]), T. Cap([7]), G. Cardella([3]), M. Colonna([1]), S. De Luca([5]), E. De Filippo([3]), D. Dell' Aquila([8]), L. Francalanza([8]), B. Gnoffo([9]), G. Lanzalone([10]), I. Lombardo([8]), C. Maiolino([1]), N. S. Martorana([1])([2]), S. Norella([5]), A. Pagano([3]), M. Papa([3]), E. Piasecki([11]), S. Pirrone([3]), G. Politi([2])([3]), F. Porto([1])([2]), L. Quattrocchi([3]), F. Rizzo([1])([2]), E. Rosato([8]), P. Russotto([3]), K. Siwek-Wilczyńska([13]), A. Trifiro([5]), M. Trimarchi([5]), G. Verde([3])([12]), M. Vigilante([8]) and J. Wilczyński([7])

([1]) *INFN, Laboratori Nazionali del Sud - Via S. Sofia, 62, Catania, Italy*
([2]) *Dipartimento di Fisica e Astronomia, Università di Catania - Via S. Sofia, 64, Catania, Italy*
([3]) *INFN, Sezione di Catania - Via S. Sofia, 64, Catania, Italy*
([4]) *Instituto de Fisica, Universidad Nacional Autonoma de Mexico - Mexico City, Mexico*
([5]) *INFN, Gruppo Collegato di Messina and Dipartimento di Fisica, Università di Messina Messina, Italy*
([6]) *Physics Faculty, University of Bucarest - Bucarest, Romania*
([7]) *National Centre for Nuclear Research - Otwock-Swierk, Poland*
([8]) *INFN, Sezione di Napoli and Dipartimento di Fisica, Università Federico II - Napoli, Italy*
([9]) *CSFNSM - Catania, Italy*
([10]) *Facoltà di Ingegneria e Architettura, Università Kore - Enna, Italy*
([11]) *University of Warsaw, Heavy Ion laboratory - Warsaw, Poland*
([12]) *Institut de Physique Nucléaire, CNRS/IN2P3 - Orsay, France*
([13]) *Faculty of Physics, University of Warsaw - Warsaw, Poland*

received 10 January 2017

Summary. — In this paper we briefly discuss about a novel application of the IMF-IMF correlation function to the physical case of binary massive projectile-like (PLF) splitting for dynamical and statistical breakup/fission in heavy ion collisions at Fermi energy. Theoretical simulations are also shown for comparisons with the data. These preliminary results have been obtained for the reverse kinematics reaction ^{124}Sn+^{64}Ni at 35 A MeV that was studied using the forward part of CHIMERA detector. In that reaction a strong competition between a dynamical and a statistical components and its evolution with the charge asymmetry of the binary break up was already shown. In this work we show that the IMF-IMF correlation function can be used to pin down the timescale of the fragments production in binary fission-like phenomena. We also made simulations with the CoMDII model in order to compare to the experimental IMF-IMF correlation function. In future we plan to extend these studies to different reaction mechanisms and nuclear systems and to compare with different theoretical transport simulations.

1. – Introduction

Two and multi particles correlation functions relevant to an intensity interferometry in a nuclear reaction at Fermi energy are useful tools in order to extract space-time information about the emission process [1]. As an example, typical analysis on proton-proton correlation functions [2] are understood in the frame of the Konin-Pratt equation [3]. Protons, indeed, are particles emitted by vastly different time scales from the pre-equilibrium to the secondary decays. However, the coexistence of dynamical and statistical mechanism in the emission of intermediate mass fragments (IMFs) is an important aspect of the reaction at intermediate energy probing in-medium particle interactions and the asymmetry term of the nuclear equation of state (ASyEOS). So it was important to extend the method of analysis by IMF-IMF correlation function studies [4-6]. First studies with CHIMERA data were done in the past for central and neck emission [7,8]. In this paper we present a preliminary work where the IMF-IMF correlation function is applied in a well-known physical case studied by the CHIMERA collaboration, that is the dynamical fission of the project-like-fragment (PLF) in ^{124}Sn+^{64}Ni at 35 A MeV reaction [9,10]. The basic idea is to provide a time-scale calibration of the IMF-IMF correlation function in a specific case and to study its evolution full shape as a function of the fission mass asymmetry.

2. – Experimental analysis

In the present paper, particles having atomic number between 3 and 25 ($3 \leq Z \leq 25$) are assigned as Intermediate Mass Fragments (IMFs). We restrict our analysis to events with IMF multiplicity equal to two ($Mult_{IMFs} = 2$). In agreement with previous studies [9,10], a constraint on the IMFs velocity, assuming that both of the two fragments had the parallel velocity greater than 5 cm/ns was implemented. Notice that the C.M. velocity of the investigated system ^{124}Sn+^{64}Ni at 35 A MeV in the laboratory frame is equal to $V_{cms} = 5.16$ cm/ns and for one of the projectile is equal to $V_{proj} = 8$ cm/ns. As it is common in CHIMERA analysis, complete events were characterized by a total detected parallel momentum greater than 60% of the projectile one and a total detected charge, Z_{tot}, (of the event) greater than 40, this assure that the PLF was almost completely detected. In order to characterize space-time properties of the IMF-IMF correlation function the selected set of IMFs was decomposed in other three set as a function of the charge asymmetry (Z_{Asy}) of the two IMFs. The asymmetry variable is defined by the ratio $Z_{Asy} = Z_H/Z_L$ where Z_H and Z_L are the atomic number of the heavy IMF and the light one, respectively. The new three sub-set are consequently labeled by: $1 \leq Z_{Asy} \leq 2$, $2 < Z_{Asy} \leq 4$ and $Z_{Asy} > 4$. In order to select IMFs coming from the PLF source another constrain was inserted in the sum of the two IMFs, such as: $25 \leq Z_H + Z_L \leq 50$. The experimental correlation function

$$[1 + R(\mathbf{V}_{\rm red})] = C_{12} \cdot \frac{Y_{coinc}(\mathbf{V}_{\rm red})}{Y_{uncor}(\mathbf{V}_{\rm red})} \tag{1}$$

is the ratio between coincident collected pairs of IMFs (in the same event) and uncorrelated ones. The denominator $Y_{uncor}(\mathbf{V}_{\rm red})$ is calculated with the event mixing tech-

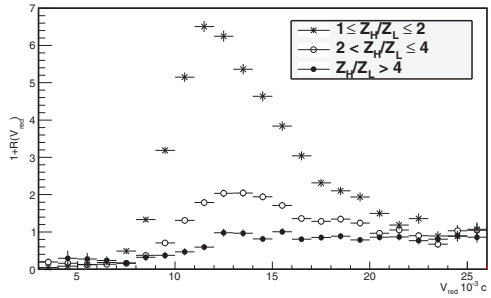

Fig. 1. – IMF-IMF correlation function for $25 \leq Z_H + Z_L \leq 50$ gated by different Z_{Asy}.

nique [11]. The IMF-IMF correlation function is calculated as a function of the reduced velocity

$$\mathbf{V}_{\rm red} = \frac{\mathbf{V}_1 - \mathbf{V}_2}{\sqrt{\mathbf{Z}_1 + \mathbf{Z}_2}} = \frac{\mathbf{V}_{\rm red}}{\sqrt{\mathbf{Z}_1 + \mathbf{Z}_2}} \tag{2}$$

in order to add together couple of particles having different atomic numbers [4]. In fig. 1 the three IMF-IMF correlation functions in the three different Z_{Asy} are shown.

The three IMF-IMF correlation functions, for the three ranges of charge asymmetry show very different shapes. It is worth to notice that the well-defined bump observed for $1 \leq Z_{Asy} \leq 2$ is centered at a value of reduced relative velocity corresponding to a binary splitting, as deduced by the Viola systematics [12]. In fig. 2 the $Z_H + Z_L$ is shown as a function of the parallel velocity of the light IMF (top panel) and in function of the parallel velocity of the heavy one (bottom panel).

Figure 2 clearly shows the tendency of the $Z_H + Z_L$ to steady decrease with the increase of the charge asymmetry of the two IMFs, indicating an increase of the energy dissipation with the increase of the charge asymmetry. Assuming that the sum $Z_H + Z_L$ is a measure of the size of the emitting source, it is argued that the shape evolution of the correlation

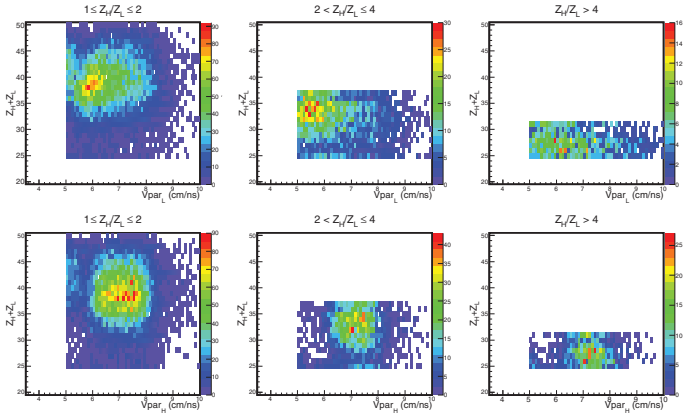

Fig. 2. – $Z_H + Z_L$ as a function of both the parallel velocity of the light IMF (top panel) and the parallel velocity of the heavy one (bottom panel) in the three ranges of Z_{Asy}.

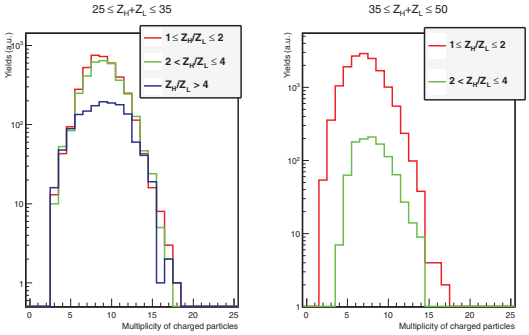

Fig. 3. – Total charged multiplicity for different Z_{Asy}, selected ranges are $25 \leq Z_H + Z_L \leq 35$ (left panel) and $35 \leq Z_H + Z_L \leq 50$ (right panel).

functions shown in fig. 1 is very poorly constrained with respect to both dissipation and size of the sources. So, in order to achieve a more careful understanding of the different shapes observed as a function of the asymmetry, it is important to compare the correlation functions by additional constrains on the size of the emitting system and the range of the energy dissipation. Consequently, we have considered two complementary narrow bins of the sum $Z_H + Z_L$, *i.e.*, one bin was defined according to the range $25 \leq Z_H + Z_L \leq 35$ and the other one $35 \leq Z_H + Z_L \leq 50$. For these two bins, the total charged particles multiplicity distributions were evaluated for the different charge asymmetries, as it is shown in fig. 3. A sizeable difference (about 3 charged particles) in the average multiplicity between the two sub-set is observed. Assuming as a crude approximation that the particle multiplicity is a reasonable indicator of the energy dissipation, fig. 3 indicates that the three charge asymmetries associated to a given size $Z_H + Z_L$ experience quite similar energy dissipation.

In the following, the IMF-IMF correlation function for the two subset values of $Z_H + Z_L$ is calculated as a function of the asymmetry. In the case of $25 \leq Z_H + Z_L \leq 35$ the different asymmetry shows remarkable differences in the shapes of the correlation functions out of the experimental error bars, fig. 4 (left panel): a well-defined bump is

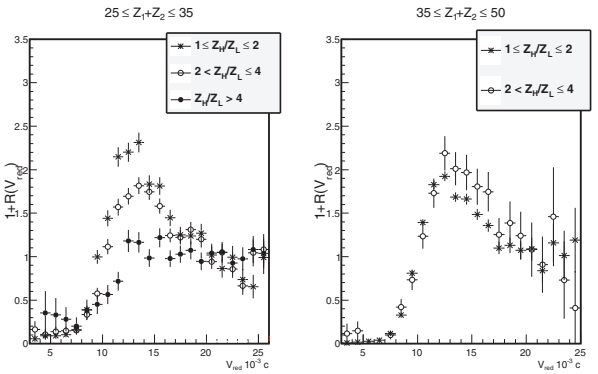

Fig. 4. – IMF-IMF correlation function for different Z_{Asy}: $25 \leq Z_H + Z_L \leq 35$ (left panel) and $35 \leq Z_H + Z_L \leq 50$ (right panel).

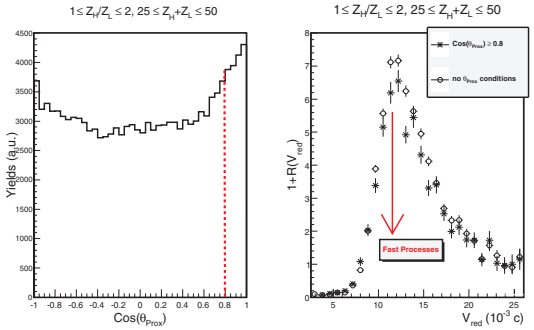

Fig. 5. – Left panel: distribution of $\cos(\theta_{prox})$ for $25 \leq Z_H + Z_L \leq 50$ and $1 \leq Z_{Asy} \leq 2$. Right panel: comparison between IMF correlation function with and without constrain in θ_{prox}.

observed for the smallest asymmetry that is progressively reduced in intensity and washed out in shape with the increase of the asymmetry. In contrast, for $35 \leq Z_H + Z_L \leq 50$ (where the smaller dissipation was observed) no significant differences have been observed within the experimental error bars, fig. 4 (right panel). The persistence of similar shapes in the binary decay process of the two IMFs is observed. Once the size of the emitting source is fixed, it is expected that the evolution of the correlation function with respect to the asymmetry characterizes the time scale of the decay process from the prompt dynamical decay (fast process) up to the equilibrated fission decay (sequential process). To support the latter observation with an independent analysis we evaluated the quantity, $\cos(\theta_{prox})$, that is a powerful indicator of the dynamical emission process for the physical case under study [13]. In brief, the theta proximity angle tells us about the angular distribution of a selected IMF for a binary splitting with respect to a well reconstructed separation axis (see ref. [13] for more details). As an example, in fig. 5 such a distribution is shown for charge symmetry $1 \leq Z_{Asy} \leq 2$ and for the full range of sizes $25 \leq Z_H + Z_L \leq 50$. In particular, forward-backward asymmetry with respect to 90° as it is seen at $\cos(\theta_{prox}) \geq 0.8$ is a signature of dynamical emission that is superimposed to a well-shaped symmetric distribution. The corresponding correlation functions are shown in the right part of fig. 5 for both the full theta proximity distribution and for $\cos(\theta_{prox}) \geq 0.8$. As you cn see (left panel of fig. 5) for the most symmetric IMFs and the range of $25 \leq Z_H + Z_L \leq 50$ the process is dominated by the statistical emission with only a few dynamical component. Even in such unfavorable case the shape of the correlation function (right panel fig. 5) when gated with the value of $\cos(\theta_{prox}) \geq 0.8$ changes and its intensity reduces toward to smaller values. That is an indication the of sensitivity of the correlation to fast emission.

3. – Theoretical comparisons

In order to pin down some quantitative information about the timescale of the dynamical process we made comparisons between the experimental data and the CoMDII model calculations [14,15]. In fig. 6 a detailed comparison between the main experimental observables used in this analysis and the ones calculated in the frame of the simulations is shown. A good agreement between experiment and simulation is observed. Notice that the simulation have been constrained as the the experimental one and the range of the resulting simulated impact parameters about $2 \leq b \leq 8$ fm was consistent with the ex-

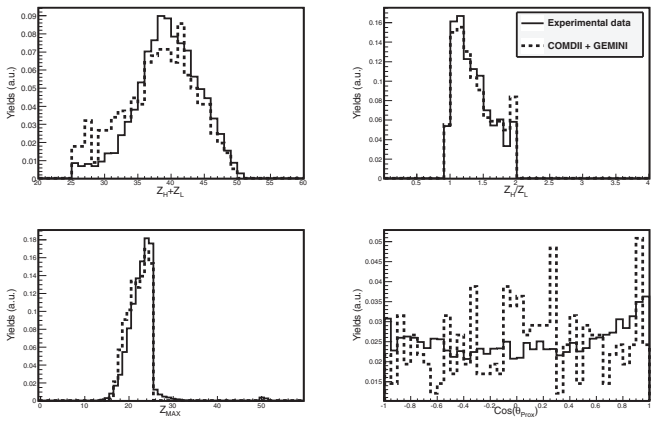

Fig. 6. – Comparisons between experimental and theoretical variables (see text for details).

perimental one, as deduced by using the Cavata method [16]. In fig. 7 the comparison between the IMF-IMF experimental correlation function (in the figure the three ranges of Z_{Asy} are reported for simplicity) and the simulated one (in red) as evaluated in the case of the most symmetric IMFs ($1 \leq Z_{Asy} \leq 2$) and for the largest range of the charge sum, ($25 \leq Z_H + Z_L \leq 50$) is shown. Notice that, at this stage, due to severe limitation of the statistic of the simulations, the comparison for larger asymmetry had, unfortunately, not shown. So further calculations have been envisaged to overcome this limitation. The calculation was stopped at 650 fm/c in order to cover the full dynamics. The final fragment distribution was obtained by using the statistical decay code Gemini [17]. Within the limitation of the present accuracy a good agreement between data and simulations is observed for the most symmetric splitting. However, it is also envisaged to compare the data with others transport models in order to obtain new information on the reaction mechanism and related time scale.

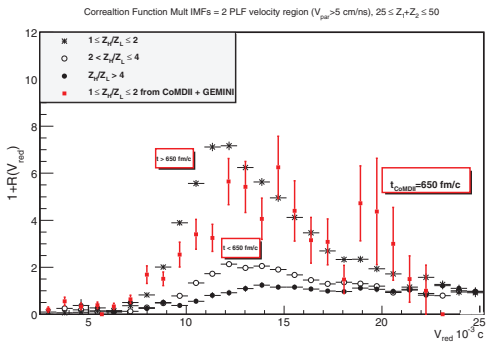

Fig. 7. – Comparisons between experimental and theoretical correlation function.

4. – Conclusions and future perspectives

This work is a preliminary study of the IMF-IMF correlation function in the specific case of dynamical PLF fission already studied for ^{124}Sn+^{64}N at 35 A MeV [10] with CHIMERA detector. The goal of this study is to be able to use the shape of the correlation function as a tool to gain information on the time scale, size and dissipative mechanism of multiple massive IMF emission (this analysis is limited to the value of Mult-IMF=2) in nuclear reactions at Fermi energies. Important source of information are expected to be available by careful comparisons of the experimental data with advanced nuclear dynamics simulations. The results discussed in the paper strongly encourage for further detailed investigations and new exciting and more exclusive experiments in this field.

REFERENCES

[1] Henzl V. *et al.*, *Phys. Rev. C*, **85** (2012) 014606.
[2] Pagano E. V., *Nuovo Cimento C*, **36** (issue 4) (2013) 9.
[3] Koonin S. E., *Phys. Lett. B*, **70** (1977) 43.
[4] DE Kim Y. D. *et al.*, *Phys. Rev. C*, **45** (1992) 338.
[5] Schapiro O., DeAngelis A. R. and Gross D. H. E., *Nucl. Phys. A*, **568** (1994) 333.
[6] Pal S., *Nucl. Phys. A*, **594** (1995) 156.
[7] Geraci E. *et al.*, *Nucl. Phys. A*, **732** (2004) 173.
[8] Maiolino C. *et al.*, *Proceedings of the XLIII International Winter Meeting on Nuclear Physics, Bormio*, edited by Iori I. and Bortolotti A., Vol. **124**, (2005) p. 194.
[9] De Filippo E. *et al.*, *Phys. Rev. C*, **71** (2005) 064604.
[10] Russotto P. *et al.*, *Phys. Rev. C*, **81** (2010) 064605.
[11] Lisa M. A., Gong W. G., Gelbke C. K. and Lynch W. G., *Phys. Rev. C*, **44** (1991) 2865.
[12] Viola V. E., Kwiatkowski K. and Walker M., *Phys. Rev. C*, **31** (1985) 1550.
[13] De Filippo E. *et al.*, *Phys. Rev. C*, **86** (2012) 014610.
[14] Papa M., Maruyama T. and Bonasera A., *Phys. Rev. C*, **64** (2001) 024612.
[15] Papa M. *et al.*, *Phys. Rev. C*, **75** (2007) 054616.
[16] De Filippo E. and Pagano A., *Eur. Phys. J. A*, **50** (2014) 32.
[17] Charity R. J., *Phys. Rev. C*, **82** (2010) 014610.